Construction of a Prognostic Nomogram Based on Autophagy-Related Genes for Children With Neuroblastoma

Evolutionary Bioinformatics
Volume 18: 1–12

DOI: 10.1177/11769343221120960
SAGE

Guogang Ye and Yue Wang

Department of General Surgery, Shanghai Children's Hospital, School of Medicine, Shanghai Jiao Tong University, Shanghai, China.

ABSTRACT: Neuroblastoma (NB) is the most common solid malignancy in children. MYCN gene amplification is the most relevant genetic alteration in patients with NB and is associated with poor prognosis. Autophagy plays specific roles in the occurrence, development, and progression of NB. Here, we aimed to identify and assess the prognostic effects of autophagy-related genes (ARGs) in patients with NB and MYCN gene amplification. Differentially expressed ARGs were identified in patients with NB with and without MYCN gene amplification, and the ARG expression patterns and related clinical data from the Therapeutically Applicable Research to Generate Effective Treatments database were used as the training cohort. Least absolute shrinkage and selection operator analyses were used to identify prognostic ARGs associated with event-free survival (EFS), and a prognostic risk score model was developed. Model performance was assessed using the Kaplan–Meier method and receiver operating characteristic (ROC) curves. The prognostic ARG mode l was verified using the validation cohort dataset, GSE49710. Finally, a nomogram was constructed by combining the ARGbased risk score with clinicopathological factors. Three ARGs (GABARAPL1, NBR1, and PINK1) were selected to build a prognostic risk score model. The EFS in the low-risk group was significantly better than that in the high-risk group in both the training and validation cohorts. A nomogram incorporating the prognostic risk score, age, and International Neuroblastoma Staging System stage showed a favorable predictive ability for EFS rates according to the area under the ROC curve at 3 years (AUC = 0.787) and 5 years (AUC = 0.787). The nomogram demonstrated good discrimination and calibration. Our risk score model for the 3 ARGs can be used as an independent prognostic factor in patients with NB and MYCN gene amplification. The model can accurately predict the 3- and 5-year survival rates.

KEYWORDS: Neuroblastoma, autophagy-related genes, prognostic model, MYCN gene amplification, nomogram, event-free survival

RECEIVED: July 1, 2022. **ACCEPTED:** July 29, 2022.

TYPE: Original Research

FUNDING: The author(s) received no financial support for the research, authorship, and/or publication of this article.

DECLARATION OF CONFLICTING INTERESTS: The author(s) declared no potential conflicts of interest with respect to the research, authorship, and/or publication of this article.

CORRESPONDING AUTHOR: Yue Wang, Department of General Surgery, Shanghai Children's Hospital, School of Medicine, Shanghai Jiao Tong University, No.355 Lu Ding Rd, Shanghai, 200040, P.R. China. Email: wangyue-njmu@163.com

Introduction

Neuroblastoma (NB) is the third leading malignant disease in children ages 0 to 14 years, after leukemia and brain cancer. It accounts for 7% of pediatric malignant tumors.[1] NB develops from neural crest precursor cells of the sympathetic nervous system. In children younger than 15 years of age, the incidence of NB is 10.54 cases per million per year.[2,3] NB is a highly malignant, rapidly progressing tumor that causes >20% of tumor-related deaths in childhood[4]; children between the ages of 18 months and 5 years are the most commonly affected. Because of the highly aggressive nature and poor prognosis associated with NB tumors, nearly half of NB cases are classified as high risk. *MYCN* gene amplification is the most relevant genetic alteration in patients with NB, as it is associated with a higher disease stage, high-risk category, tumor aggressiveness, and poor prognosis.[5] Unfortunately, approximately one quarter of patients with NB have *MYCN* gene amplification, and some scholars have proposed that *MYCN* gene amplification is a biomarker of poor prognosis in these patients and is an attractive therapeutic target for the treatment of NB.[5,6]

Autophagy is a process in which cells use autophagosomes to degrade their macromolecular substances or damaged organelles under the regulation of various external stimuli and autophagy-related genes (ARGs).[7] The autophagy process can degrade nonfunctional organelles and recycle their components, which may contribute to supplying the demands of tumor invasion and development.[8,9]

Belounis et al[10] reported that chemotherapy induces autophagy associated with survival in NB cells, contributing to apoptosis suppression and chemoresistance. Tanimoto et al[11] demonstrated that the telomerase-targeted oncolytic adenoviruses OBP-301 and OBP-702 exhibited strong antitumor effects in association with autophagy in *MYCN*-amplified NB cells via *MYCN* suppression. Dong et al[12] investigated a combination of rapamycin and MK-2206 for the treatment of high-risk patients with NB and *MYCN* amplification and indicated that autophagy and necroptosis that mediated cell death induced by the combination of rapamycin and MK-2206 were *MYCN* dependent.

Many scholars have discussed the correlation between ARGs and the occurrence, development, or spontaneous regression of NB.[12-15] However, studies using large-scale ARG expression profiles to investigate the relationship between the prognosis of patients with NB, *MYCN* gene amplification, and ARGs are lacking.

In this study, ARG expression profiles and clinical prognostic data from patients with NB and *MYCN* gene amplification were analyzed by data mining and bioinformatics analysis of gene expression profiles to establish a risk score model for the prediction of clinical outcomes.

Methods

Data collection

All 232 human ARGs were selected from the Human Autophagy Database (HADb, http://www.autophagy.lu/index.html). Data from 68 *MYCN*-amplified and 175 *MYCN*-nonamplified NB samples, including mRNA sequencing and clinical information, were extracted from the Therapeutically Applicable Research to Generate Effective Treatments (TARGET) database (https://ocg.cancer.gov/). Moreover, the GSE49710 dataset was downloaded, which included 92 *MYCN*-amplified and 401 *MYCN*-nonamplified NB samples from the Gene Expression Omnibus (GEO) database. In summary, 243 samples downloaded from the TARGET database served as the training cohort, and 493 samples from the GSE49710 dataset were used as the validation cohort. Because all data were collected from publicly available datasets in the HADb, TARGET, and GEO databases, approval from an ethics committee was not required.

Screening and functional enrichment analysis of differentially expressed ARGs

Expression data from 232 ARGs in 243 NB samples were obtained, and $\log_2$ mean values were calculated, to generate standardized expression values. The Wilcoxon signed-rank test in R (version 3.6.1, https://www.r-project.org/) was used to identify 18 ARGs that were differentially expressed between *MYCN* gene-amplified and *MYCN gene*-nonamplified samples. The threshold was set as | log (fold change) | >1 and a false discovery rate <0.05. Continuous data were compared using Student's *t*-test or Wilcoxon's signed-rank test using R software (version 3.5.0, R Foundation for Statistical Computing).

The biological functions of differentially expressed ARGs were analyzed using Gene Ontology (GO) and the "clusterProfiler" package in R/Bioconductor.[16] The Kyoto Encyclopedia of Genes and Genomes (KEGG) was used to analyze pathways enriched for differentially expressed ARGs. Gene set enrichment analysis (GSEA) was used to analyze the pathways enriched for differentially expressed DEGs. The threshold for enrichment analysis was $P < .05$.

Establishment and validation of an ARG prognostic model

The least absolute shrinkage and selection operator (LASSO) analyses were used to identify the ARGs associated with event-free survival (EFS) in patients with NB. The expression values of each gene were combined, regression coefficients were obtained by LASSO weighted analysis, and a risk score formula was constructed for patients with NB.

The ARG-based prognostic risk score model[17] was calculated as follows:

$$Risk\ score = \sum_{i=1}^{n} vi \times ci$$

where *vi* represents the expression value of differentially expressed ARGs, *ci* is the regression coefficient of gene *i* obtained by Lasso analysis, and *n* is the quantum of independent indicators obtained by Lasso analysis.

The total risk score for each sample was obtained according to this formula, and all NB samples were assigned to low- and high-risk groups according to the median risk score. Kaplan-Meier analysis was used to evaluate differences in survival between the 2 groups, and the log-rank method was applied to assess the significant differences in survival between the 2 groups. Receiver operating characteristic (ROC) curves were used to assess the predictive value of the prognostic risk model.[18] The GSE49710 dataset served as a validation cohort and was analyzed using the same method as the training cohort to obtain a total risk score for each sample. The predictive ability of the ARG-based prognostic risk score model was assessed using the Kaplan-Meier survival curve analysis.

Clinical application

Univariate and multivariate Cox analyses were conducted to determine the clinical performance of the prognostic score model, whether the model was independent of other clinicopathological parameters (including sex, age, *MYCN* amplification status, DNA ploidy status, mitosis-karyorrhexis index (MKI), pathological histology results, Children's Oncology Group [COG] risk group, and International Neuroblastoma Staging System [INSS] stage), and whether the model could be used to assess the prognosis of patients with NB. According to the results of the multivariate Cox analysis, a nomogram was established to predict the 3- and 5-year survival probabilities of patients with NB. C-index values and calibration plots were used to assess the discriminative performance and discriminative ability of the nomogram.[19] Statistical analysis was performed using SPSS 22.0 (Chicago, IL, USA), and continuous data were compared using Student's *t*-test or Wilcoxon's rank test. Categorical data were expressed as a number and compared using the chi-square or Fisher's exact tests. Kaplan-Meier analysis and log-rank method were also applied.

Statistical analyses

Comparisons of quantitative variables were performed using Student's *t*-test (normally distributed data) or Wilcoxon's rank test (non-normally distributed data), and analysis of categorical variables was conducted using the chi-square or Fisher's exact test. The Kaplan-Meier survival curves of patients in the low- and high-risk groups were plotted, and log-rank tests were used to evaluate differences between the 2 groups. A risk score formula was established based on the Lasso regression coefficient and the gene expression values. According to the results of the multivariate analysis using the "rms" package in R, a nomogram was established, and area under the ROC curve (AUC) values were calculated using the "survivalROC" package in R to evaluate the predictive value of the nomogram. Calibration plots were drawn to compare the predicted and observed survival rates. All data were analyzed using SPSS 22.0 (Chicago, IL, USA) and R software (version 3.6.1). *P*-values of ⩽.05 were considered statistically significant.

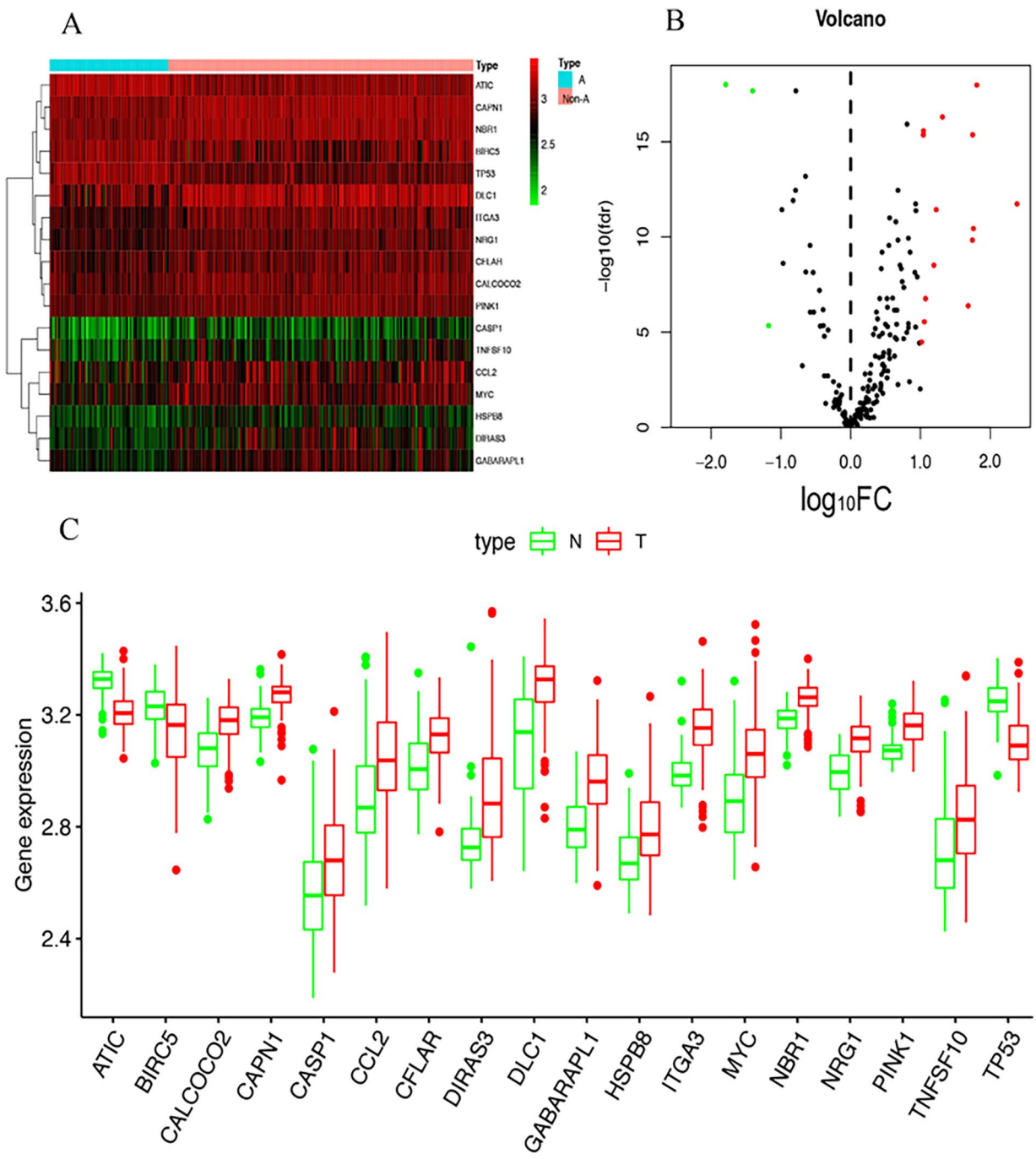

Figure 1. Comparison of autophagy-related genes (ARGs) differentially expressed between MYCN-amplified and MYCN-nonamplified neuroblastoma (NB) groups: (A) heat map for 18 differentially expressed ARGs between the MYCN-amplified and MYCN-nonamplified groups, (B) volcano plot of 232 ARGs in NB cases from the TARGET database, and (C) box plots for 18 ARGs differentially expressed in the MYCN-amplified and MYCN-nonamplified groups.

Results

Determination of ARGs differentially expressed between MYCN-amplified and MYCN-Nonamplified NB

Data from 243 patients with NB were included in our study. All patient data had complete RNA sequencing and clinical follow-up information. Using a threshold of $|\log_2$ fold change$| > 1$, 18 DEGs were screened from 232 ARGs, including 15 that were upregulated (*CALCOCO2*, *CAPN1*, *CASP1*, *CCL2*, *CFLAR*, *DIRAS3*, *DLC1*, *GABARAPL1*, *HSPB8*, *ITGA3*, *MYC*, *NBR1*, *NRG1*, *PINK1*, and *TNFSF10*) and 3 downregulated genes (*ATIC*, *BIRC5*, and *TP53*) (Figure 1A). Volcano and box plots were used to illustrate the differences in ARG expression between the *MYCN* gene-amplified and *MYCN*-nonamplified groups (Figure 1B and C). The clinicopathological characteristics of all patients with NB are presented in Supplemental Material 1.

Enrichment analysis of differentially expressed ARGs

To understand the biological functions of the 18 differentially expressed ARGs, functional enrichment analysis was conducted.

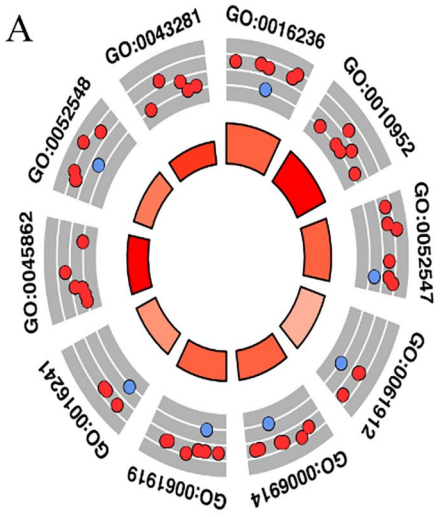

ID	Description
GO:0016236	macroautophagy
GO:0010952	positive regulation of peptidase activity
GO:0052547	regulation of peptidase activity
GO:0061912	selective autophagy
GO:0006914	autophagy
GO:0061919	process utilizing autophagic mechanism
GO:0016241	regulation of macroautophagy
GO:0045862	positive regulation of proteolysis
GO:0052548	regulation of endopeptidase activity
GO:0043281	regulation of cysteine–type endopeptidase activity involved in apoptoti

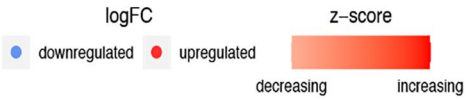

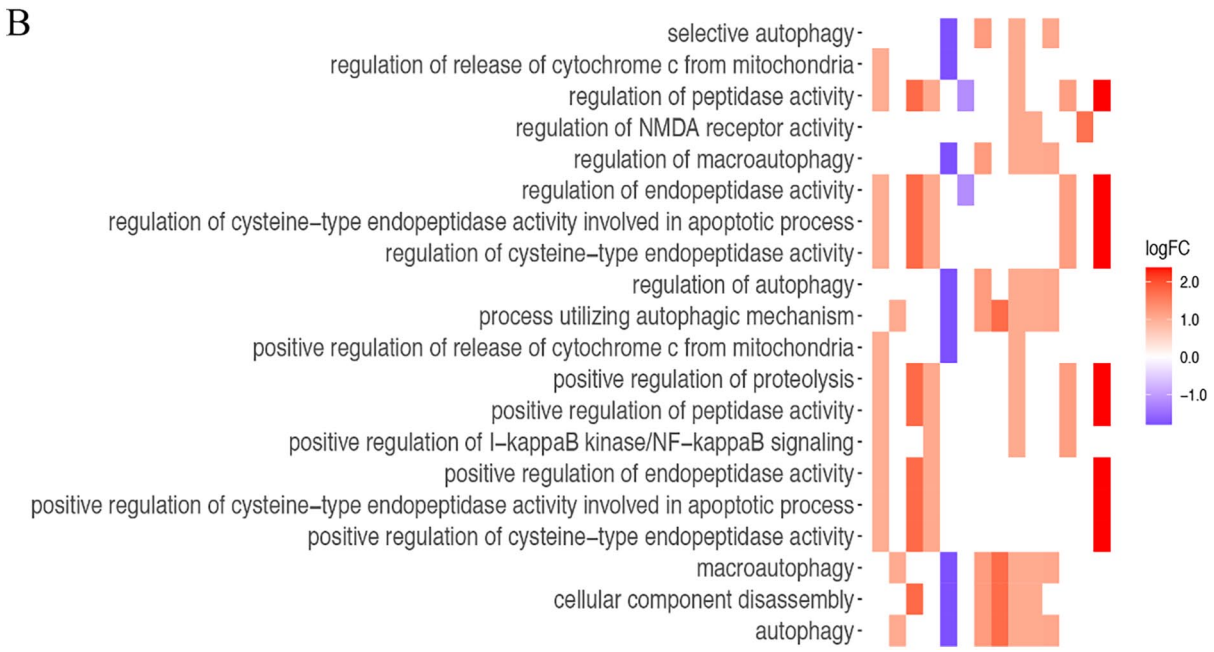

Figure 2. Gene ontology functional enrichment analysis for autophagy-related genes (ARGs) differentially expressed in neuroblastoma tissues: (A) circle plot showing differentially expressed ARGs and biological processes and (B) heat map showing differentially expressed ARGs and biological processes.

The results demonstrated that the biological processes involving DEGs were primarily macroautophagy, regulation of peptidase activity, positive regulation of peptidase activity, and selective autophagy. The main pathways identified by KEGG enrichment analysis were mitophagy-animal, apoptosis, shigellosis, and necroptosis. The results of the GO analysis for differentially expressed ARGs are illustrated as circles and heat maps (Figure 2A and B), as are the results of the KEGG enrichment analysis for differentially expressed ARGs (Figure 3A and B). The main pathways identified by GSEA for DEGs were apoptosis, shigellosis, influenza A, thyroid cancer, and NOD-like receptor signaling pathway; the results of GSEA are illustrated in Figure 3C.

Identification of prognosis-related ARGs and construction of a prognostic risk model

Lasso analysis identified 3 genes, *GABARAPL1*, *NBR1*, and *PINK1*, and a prognostic risk score model was constructed based on the expression levels and regression coefficients of

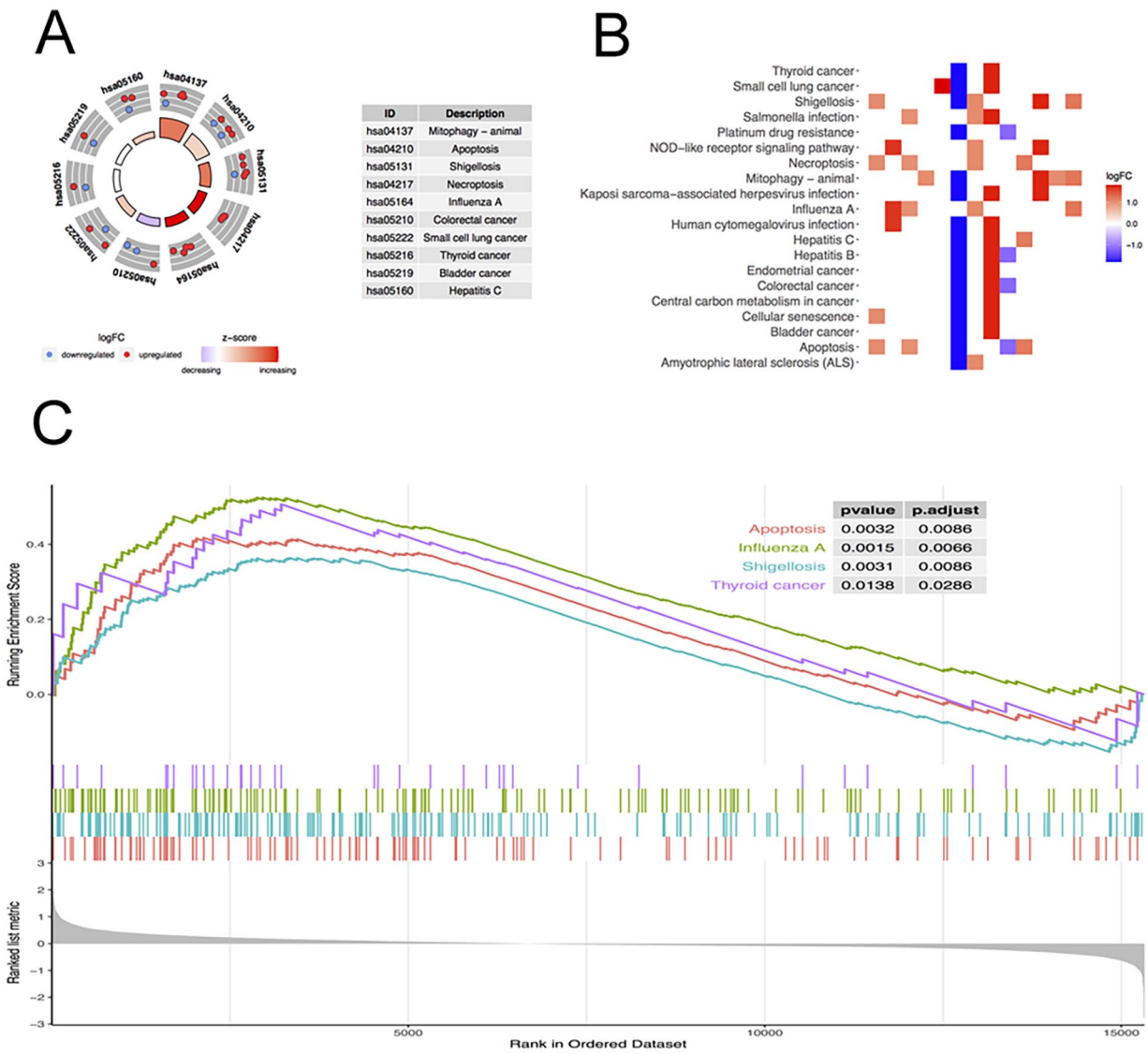

Figure 3. Functional enrichment analysis of autophagy-related genes (ARGs) differentially expressed in neuroblastoma tissues: (A) circle plot showing differentially expressed ARGs and Kyoto Encyclopedia of Genes and Genomes (KEGG) pathways, (B) heat map showing differentially expressed ARGs and KEGG pathways, and (C) main pathways identified by gene set enrichment analysis (GSEA) for differentially expressed genes.

each gene (Figure 4A and B). The prognostic risk score model was as follows:

Risk score = (−0.0078 × expression value of *GABARAPL1*) + (−0.3386 × expression value of *NBR1*) + (−0.1703 × expression value of *PINK*)

The total risk scores were calculated for each patient, and all patients with NB in the training cohort were divided into the low- and high-risk groups according to the median risk score value (Figure 5A).

The Kaplan-Meier survival analysis demonstrated that the EFS of patients with low-risk scores was significantly better than that those with high-risk scores in the training cohort ($P = 9.776 \times 10^{-5}$) (Figure 6A). The 3-year EFS probabilities of patients in the low- and high-risk groups were 59.6% (95% CI: 0.514-0.691) and 33.1% (95% CI: 0.255-0.430), respectively, whereas the corresponding 5-year EFS probabilities were 55.0% (95% CI: 0.467-0.648) and 30.8% (95% CI: 0.233-0.407), respectively. The C-index for the prognostic risk model to predict EFS in patients with NB was 0.666 (95% CI: 0.698-0.736) (Figure 6B); the AUC values for 3- and 5-year survival were 0.681 and 0.689, respectively (Figure 6C).

Using the median expression level of each gene in patients with NB as cutoff points, high expression levels of *GABARAPL1* (hazard ratio [HR] = 0.706; 95% CI, 0.560-0.888; $P = .015$), *NBR1* (HR = 0.504; 95% CI, 0.350-0.725; $P = 2.469 \times 10^{-4}$), and *PINK1* (HR = 0.533; 95% CI, 0.362-0.786; $P = 2.897 \times 10^{-4}$) were associated with better EFS (Figure 7A–C).

Evaluation of the prognostic risk model in an external cohort

The prognostic value of the ARG-based risk score model built using TARGET cohort data was validated using an approach similar to that of the GSE49710 dataset. All 493 patients with

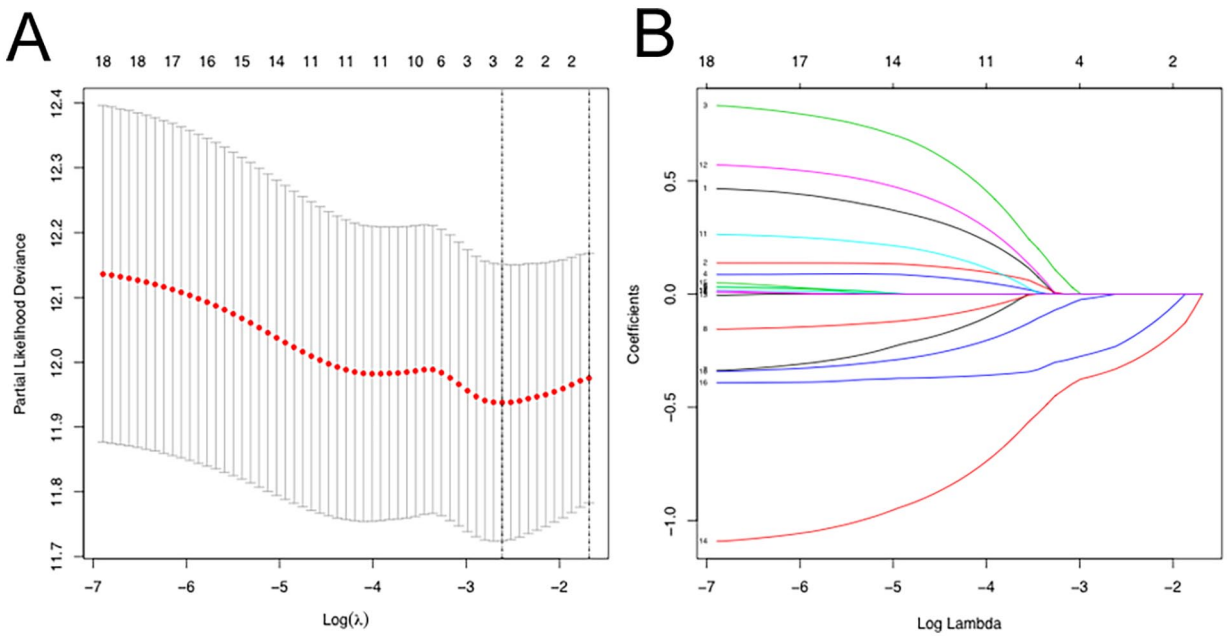

Figure 4. Eighteen genes selected using LASSO binary logistic regression analysis: (A) tuning parameter (λ) selection using tenfold cross-validation via minimum criteria to select the best penalty parameter lambda and (B) LASSO coefficient profiles of 18 genes.

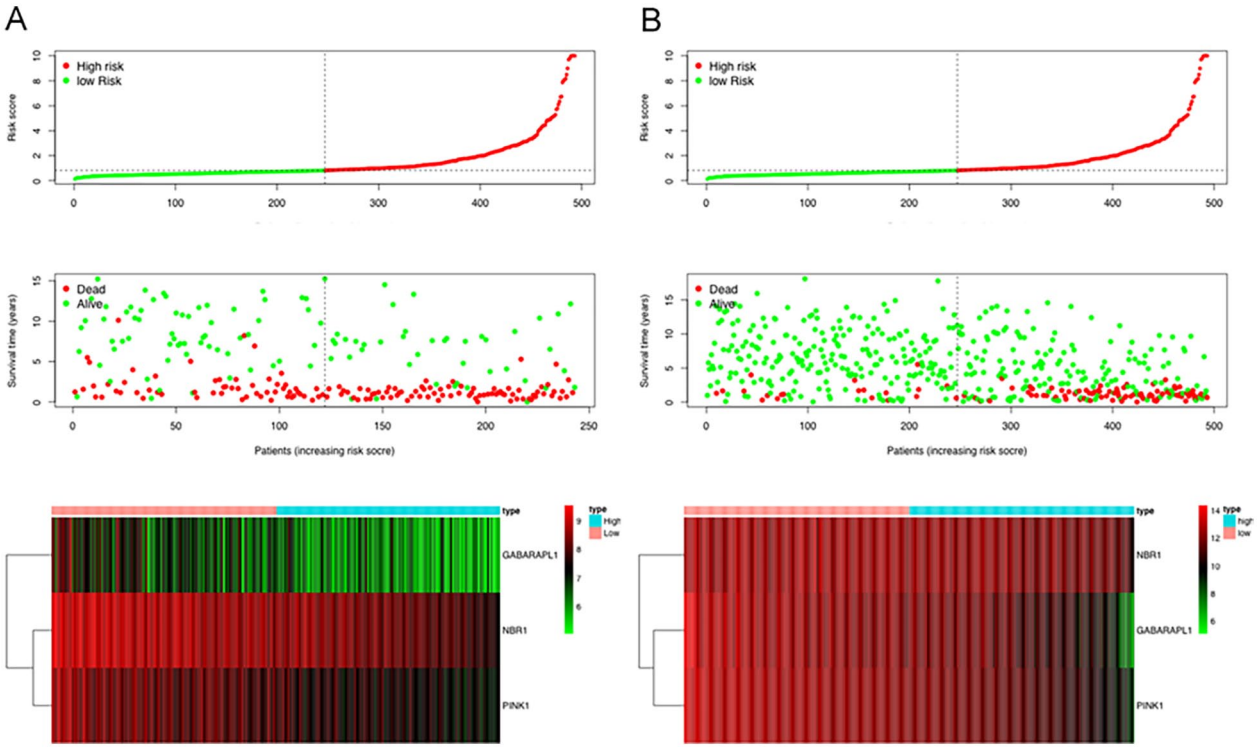

Figure 5. Risk score plots of patients with high- and low-risk neuroblastoma (NB). Risk score plots of patients with NB in the high- and low-risk groups in the (A) training and (B) validation cohorts.

NB in the GSE49710 dataset were divided into the low-risk (n = 247) and high-risk (n = 246) groups according to the median risk score generated using our model.

As shown in Figure 5B, the EFS of patients with low-risk scores was significantly better than those with high-risk scores in the validation cohort ($P = 1.799 \times 10^{-14}$) (Figure 6D). The 3-year EFS probability of patients in the low-risk group was 92.0% (95% CI: 0.885-0.956), whereas those in the high-risk group was 60.9% (95% CI: 0.546-0.679). The 5-year EFS probability of patients in the low-risk group was 90.8% (95% CI: 0.870-0.947); however, the 5-year EFS probability of those in the high-risk group was low, possibly because the 5-year

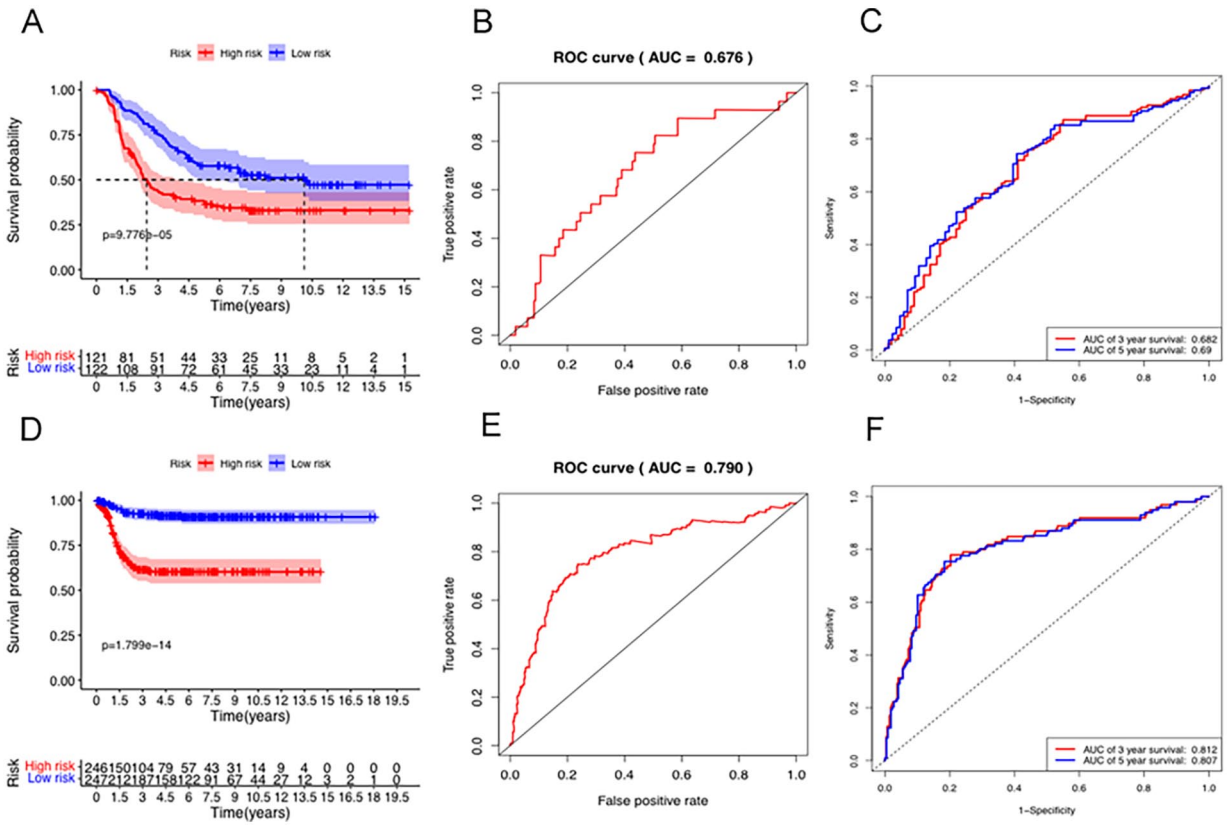

Figure 6. Kaplan-Meier survival curves of patients with NB in the high- and low-risk groups in the (A) training and (D) validation cohorts. Receiver operating characteristic (ROC) curves for the overall survival related prognostic risk score model of patients with NB in the (B) training and (E) validation cohorts. ROC curves for the 3- and 5-year survival rates in the (C) training and (F) validation cohorts.

EFS time in the high-risk group in this cohort was <5 years. The C-index of the prognostic risk score model for the prediction of EFS in patients with NB was 0.790 (95% CI: 0.814-0.846) (Figure 6E). Furthermore, the AUC values for the 3- and 5-year survival were 0.812 and 0.807, respectively (Figure 6F).

Using the median expression level for each gene in the GSE49710 dataset as a cutoff point, high expressions of *GABARAPL1* (HR = 0.608; 95% CI, 0.549-0.672; $P = 1.535 \times 10^{-13}$), *NBR1* (HR = 0.401; 95% CI, 0.301-0.533; $P = 5.525 \times 10^{-9}$), and *PINK1* (HR = 0.457; 95% CI, 0.387-0.541; $P = 1.477 \times 10^{-13}$) were associated with better EFS (Figure 7D–F).

Relationships between clinicopathological parameters and ARG prognostic risk score model

The demographic and clinicopathological features of all patients with NB are presented in Supplemental Material 1. The relationships between the ARG-based prognostic risk scores and clinicopathological characteristics were analyzed.

EFS-related prognostic risk score values were higher in patients aged ⩾18 versus <18 months ($P = 8.560 \times 10^{-13}$); in patients with undifferentiated versus differentiated tumors ($P = 2.032 \times 10^{-4}$); in the high-risk versus low-risk group (as grouped by the COG risk group) ($P = 1.455 \times 10^{-16}$); in the high- and intermediate-risk groups versus the low-risk group (as grouped by MKI) ($P = 1.310 \times 10^{-8}$); in patients with stage 4 versus stages 1, 2, and 3 disease ($P = 8.172 \times 10^{-12}$); in patients with diploid (DNA index [DI] = 1) versus hyperdiploid (DI > 1) status ($P = .003$); in patients with *MYCN*-amplified versus *MYCN*-nonamplified status ($P = 3.157 \times 10^{-18}$); and in the unfavorable versus favorable group ($P = 7.166 \times 10^{-16}$) in the training cohort (Figure 8A–H). EFS-related prognostic risk score values were also higher in patients aged ⩾18 versus <18 months ($P = 5.355 \times 10^{-10}$); in *MYCN*-amplified versus *MYCN*-nonamplified disease ($P = 1.106 \times 10^{-16}$); in high-risk versus low-risk patients ($P = 4.33 \times 10^{-19}$); and in patients with stage 4 versus stages 1, 2, and 3 disease ($P = 1.693 \times 10^{-11}$) in the validation cohort (Figure 8I–L). Among the 493 patients with NB in the validation cohort, data on tumor grade, MKI, and histology were lacking; therefore, the relationship between these factors and the prognostic risk score could not be analyzed.

Univariate Cox analyses showed that age ($P < .001$), *MYCN* status ($P < .001$), ploidy ($P < .001$), MKI ($P < .05$), COG risk group ($P < .05$), and prognostic risk score ($P < .001$) were significantly correlated with EFS (Figure 9A). Furthermore, multivariate Cox analyses showed that age ($P < .001$), INSS stage ($P = .02$), and prognostic risk score ($P = .02$) were significantly associated with EFS (Figure 9B).

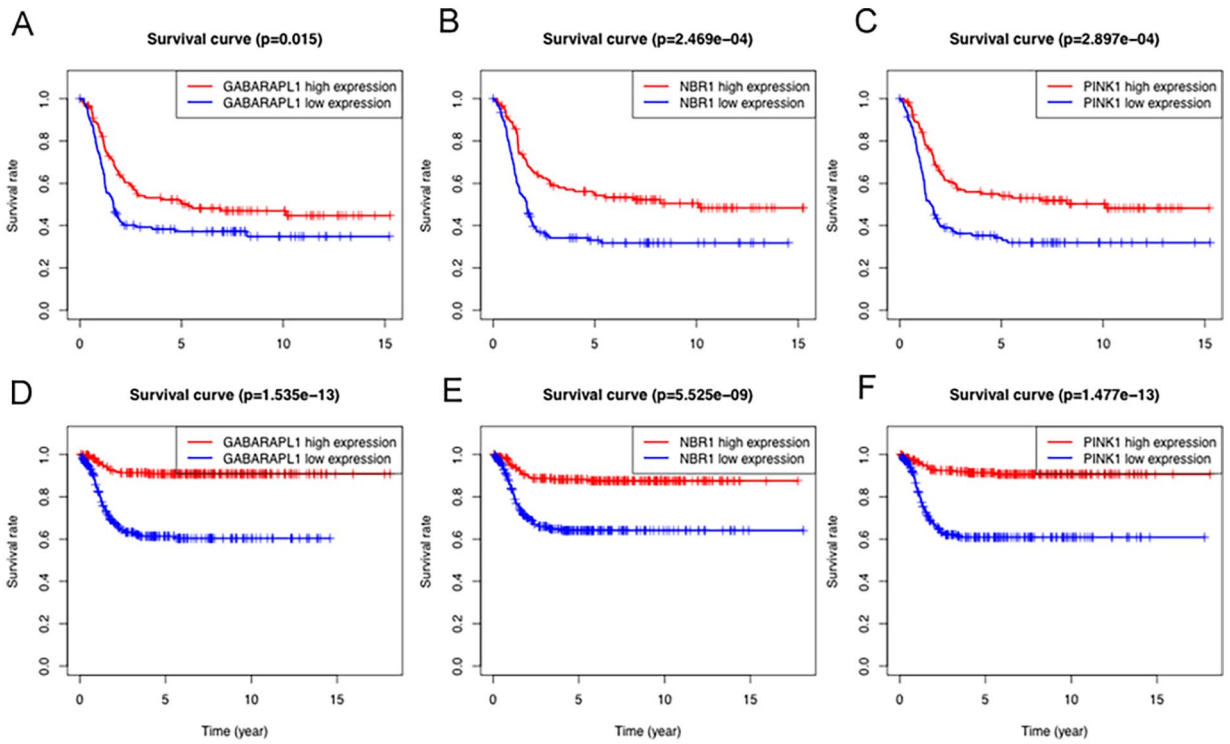

Figure 7. Survival analysis according to GABARAPL1, NBR1, and PINK1 expression levels in the (A–C) training and (D–F) validation cohorts. Kaplan-Meier event-free survival (EFS) curves based on the expression levels of (A) GABARAPL1, (B) NBR1, and (C) PINK1 in patients with neuroblastoma (NB) in the training cohort. Kaplan-Meier EFS curves based on expression levels of (D) GABARAPL1, (E) NBR1, and (F) PINK1 in patients with NB in the validation cohort.

Establishment and internal validation of a prognosis nomogram

To establish a clinical method that could simply and rapidly predict the prognosis of patients with NB, we established a prognostic nomogram to predict the 3- and 5-year survival probabilities of patients with NB using training cohort data and conducted an internal validation of the nomogram. The prognostic risk score, age, and INSS stage were the 3 independent prognostic parameters used to construct the nomogram to predict the prognosis of patients with NB (Figure 10A). The C-index of the nomogram in predicting EFS in patients with NB was 0.745 (95% CI, 0.716-0.770; $P = 1.91 \times 10^{-7}$) (Figure 10B), and the AUC values for the 3- and 5-year survival were 0.787 and 0.787, respectively (Figure 10C). The nomogram could accurately predict the 3- and 5-year survival probabilities of patients with NB, and calibration plots showed that the predicted survival rates were very close to the observed rates (Figure 10D and E).

Discussion

NB remains a large social and economic burden for many individuals and countries because of its high recurrence rate, cost, and mortality rate. In the past 10 years, high-throughput biotechnology has been widely used to diagnose various tumors and, in particular, to identify gene markers for NB. The *MYCN* was one of the gene markers, that show patients with *MYCN* amplification are associated with a high risk and worse prognostic outcome.[20] Autophagy plays a critical role in the occurrence and development of NB.[21,22] However, to our knowledge, the association between ARGs and *MYCN* gene amplification in NB has not been fully explored. Therefore, we established an association between ARGs and *MYCN* gene amplification in the current study.

First, we identified 18 differentially expressed ARGs using data from 243 NB samples. Next, we used GO, KEGG, and GSEA pathway analyses to assess the biological functions of differentially expressed ARGs. In addition, using valid gene data from patients with NB in the TARGET database, we screened and identified 3 ARGs that could serve as key prognostic genes and used them to construct an ARG-based prognostic risk score model. Validation of the performance of the prognostic risk score model using the GSE49710 dataset demonstrated that the model had a very good ability to predict the prognosis of patients with NB. Finally, we successfully constructed a prognostic nomogram based on the clinical risk score and clinicopathological factors. The discrimination and accuracy of the nomogram in predicting the prognosis of patients with NB were validated using discriminant and calibration plots.

All patients with NB were divided into low- and high-risk groups, using the median risk score from the 3-ARG prognostic risk model as a cutoff value. Compared with patients with high-risk scores, those with low-risk scores had significantly

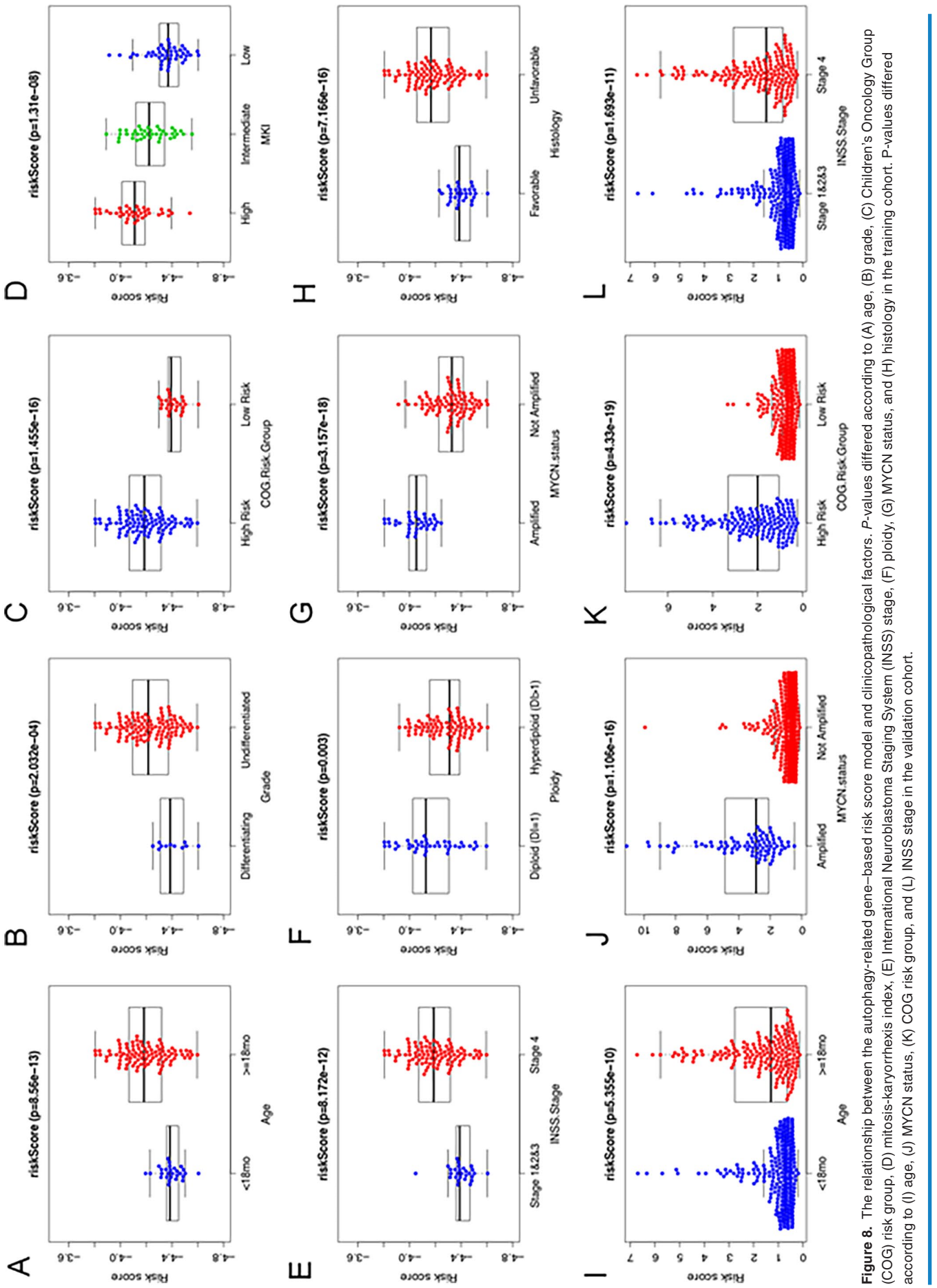

Figure 8. The relationship between the autophagy-related gene–based risk score model and clinicopathological factors. *P*-values differed according to (A) age, (B) grade, (C) Children's Oncology Group (COG) risk group, (D) mitosis-karyorrhexis index, (E) International Neuroblastoma Staging System (INSS) stage, (F) ploidy, (G) MYCN status, and (H) histology in the training cohort. P-values differed according to (I) age, (J) MYCN status, (K) COG risk group, and (L) INSS stage in the validation cohort.

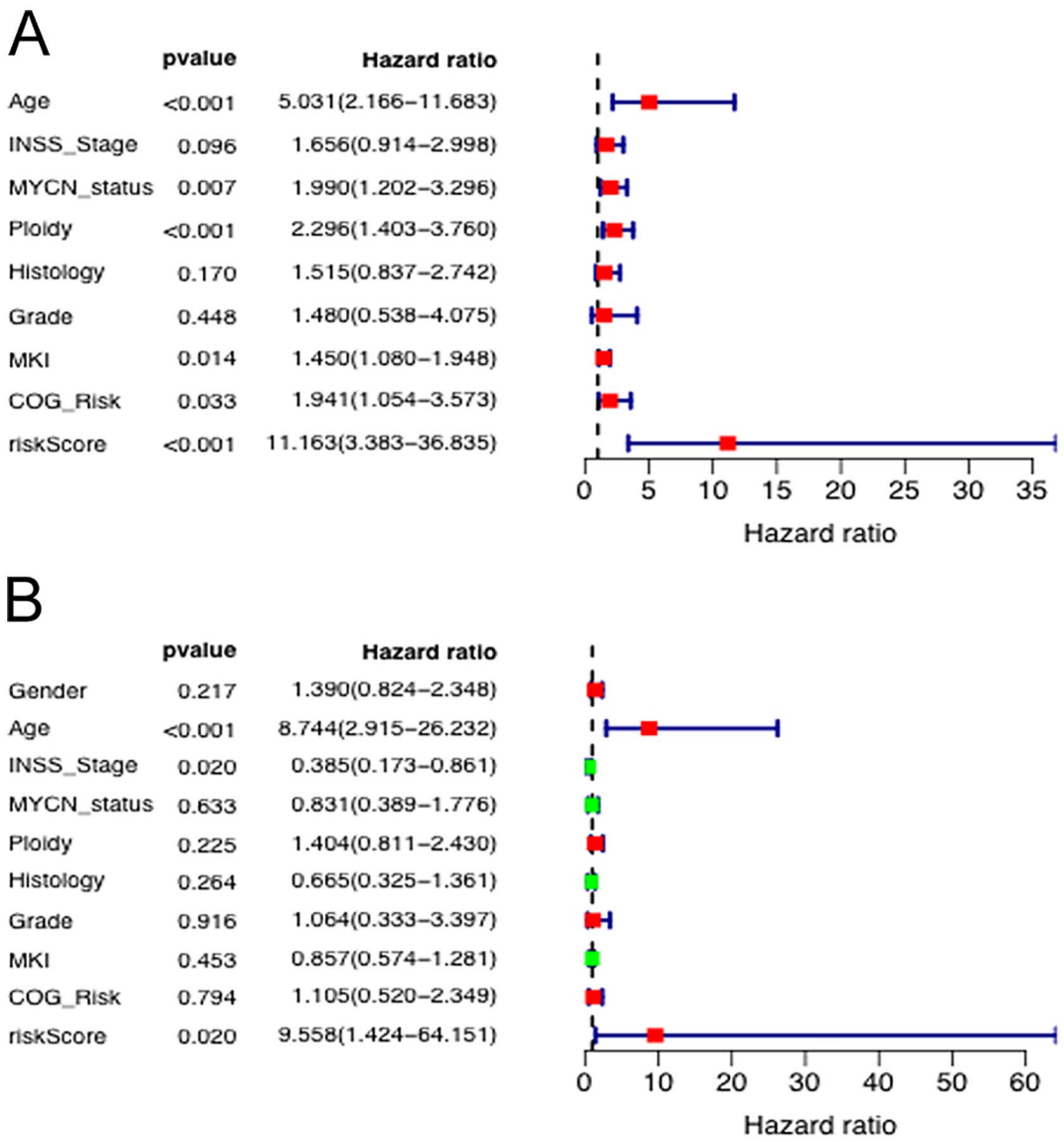

Figure 9. Risk forest plots for the autophagy-related gene–based risk score model and clinicopathological factors by (A) univariate and (B) multivariate Cox regression analyses.

longer 3- and 5-year EFS. Hence, more accurate personalized treatment strategies should be established for patients with high-risk scores according to their characteristics. All patients with high-risk scores should receive more aggressive treatment and closer follow-up to ensure the timely detection of tumor recurrence.

Our ARG-based prognostic risk score model could predict the prognosis of patients with NB. *GABARAPL1* has a tumor-suppressive function. Loss of *GABARAPL1* expression has been correlated with poor survival and advanced stages of neuroblastoma,[23] which is consistent with our findings. Meng et al[15] built an ARG-based prognostic risk signature using 9 ARGs in patients with NB with stages 4 and 4seconds. *GABARAPL1* was highly expressed in the low-risk group and was associated with good overall survival, which is consistent with the results of our study, although Meng et al[15] focused on the role of autophagy in the specific phenomenon of spontaneous regression of neuroblastoma.

However, little is known about the role of *NBR1* in cancer prognosis. Xiao et al[24] reported that low mRNA levels of NBR1 were associated with poor clinical outcomes in patients with clear cell renal carcinoma. Recent studies have shown that autophagic degradation of NBR1 inhibits metastatic growth by limiting an aggressive basal subset of tumor cells, and that NBR1 is a key determinant in the regulation of tumor cell heterogeneity and metastatic disease, suggesting that induction of autophagic degradation of NBR1 is a therapeutic approach to prevent the recurrence of life-threatening metastases.[25,26]

PINK1, known as a sensor of mitochondrial dysfunction, has been purported to have a dual role in cancer biology, with context-dependent pro- and antitumorigenic properties.[27] Li et al[28] demonstrated that *PINK1* and *PARK2* suppressed pancreatic tumorigenesis through the control of mitochondrial iron-dependent immunometabolism. In colorectal cancer, it has been shown that mitophagy protein PINK1 suppresses colon tumor growth by metabolic reprograming and reduces

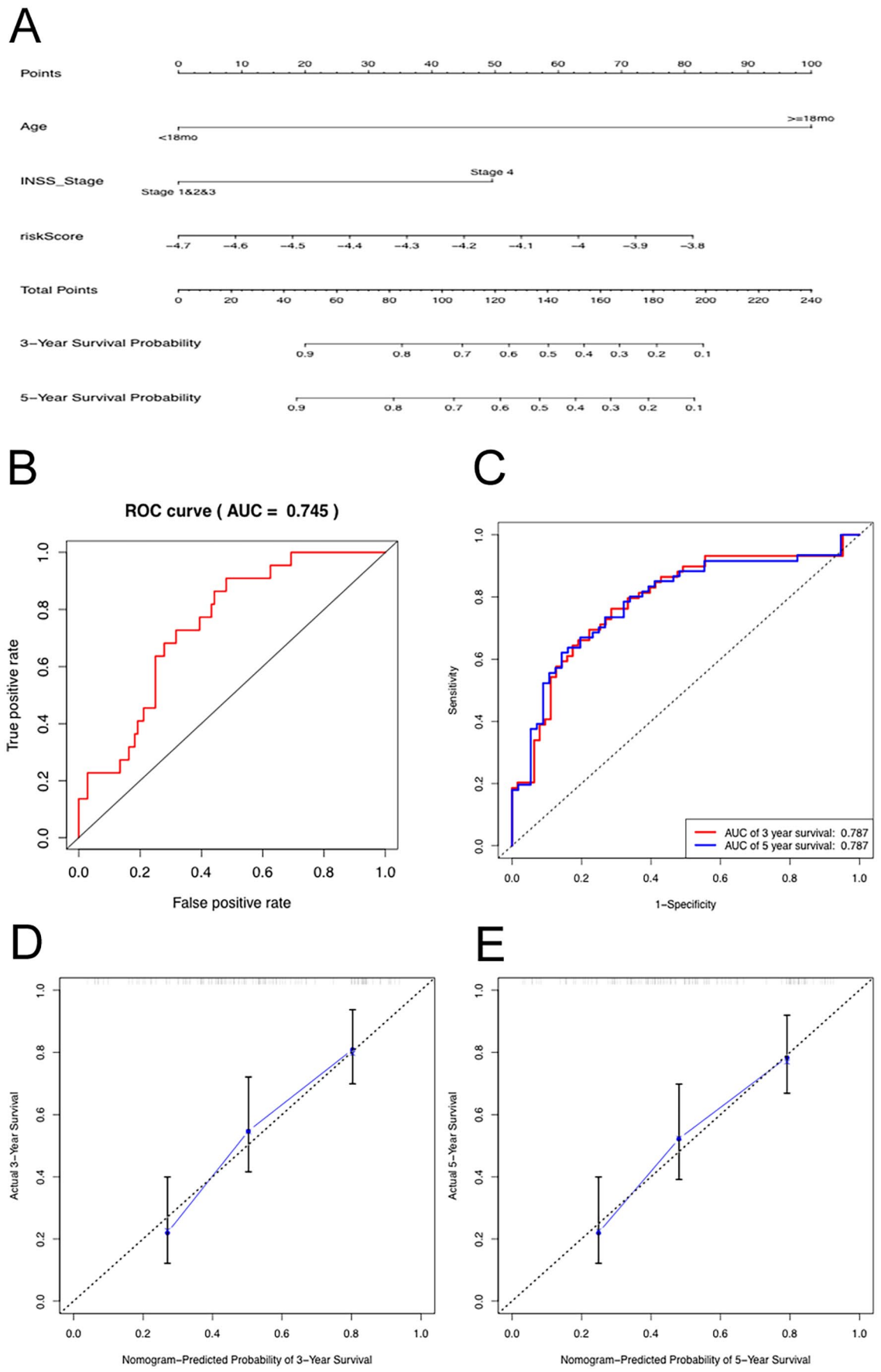

Figure 10. (A) Nomogram to predict the 3- and 5-year survival probabilities of patients with NB. (B) Receiver operating characteristic (ROC) curves for the event-free survival (EFS)–related prognostic risk score model of patients with NB in the training cohorts. (C) ROC curves for the nomogram to predict the 3- and 5-year survival probabilities of patients with NB in the training cohort. Calibration curves for the nomogram to predict (D) 3- and (E) 5-year survival probabilities of patients with NB in the training cohort.

acetyl-CoA production.[29] Similarly, low expression of *PINK1* was significantly related to higher tumor stage, and positive nodal status was an independent prognostic factor for overall survival in papillary renal cell carcinoma.[30] Conversely, *PINK1* expression is reportedly upregulated in lung cancer, which promotes cell migration and proliferation and predicts a poor prognosis.[31] Unlike *GABARAPL1*, *NBR1*, and *PINK1* are rarely studied in NB, and additional studies are needed.

Nomograms are increasingly used by clinicians because of their simplicity, convenience, and directness. In this study, we constructed a nomogram incorporating prognostic risk score, age, and INSS stage. Calibration plots based on TARGET cohort data showed that 3- and 5-year EFS predicted by the nomogram were closely related to the observed EFS, indicating that the nomogram will have excellent performance in predicting 3- and 5-year EFS in patients with NB. This convenient and intuitive nomogram can help both clinicians and patients to make personalized survival predictions, which will help in the selection of appropriate and personalized treatment options. Because some clinical information from the GSE49710 database was incomplete, we only internally validated the nomogram accuracy.

This study has some limitations. First, the nomogram we constructed lacked external validation; therefore, to ensure its robustness, the nomogram should be validated externally. Second, all data included in this study were downloaded from databases, and all analyses were theoretical; hence, some functional experiments should be conducted to explore the molecular mechanisms underlying the relationships between these 3 ARGs and NB occurrence, metastasis, and prognosis. For this prognostic prediction model to be more widely applicable to patients with NB, its accuracy requires additional validation in prospective, multicenter, and large-scale clinical trials.

Conclusion

In summary, we successfully constructed a reliable nomogram that could accurately predict the 3- and 5-year survival probabilities of patients with NB and *MYCN* gene amplification. This model facilitates the implementation of more accurate and personalized treatment strategies for patients with this disease.

ORCID iD

Yue Wang https://orcid.org/0000-0001-6636-354X

Supplemental Material

Supplemental material for this article is available online.

REFERENCES

1. Salazar BM, Balczewski EA, Ung CY, Zhu S. Neuroblastoma, a paradigm for big data science in pediatric oncology. *Int J Mol Sci*. 2016;18:37.
2. Gurney JG, Ross JA, Wall DA, Bleyer WA, Severson RK, Robison LL. Infant cancer in the U.S.: histology-specific incidence and trends, 1973 to 1992. *J Pediatr Hematol Oncol*. 1997;19:428-432.
3. London WB, Castleberry RP, Matthay KK, et al. Evidence for an age cutoff greater than 365 days for neuroblastoma risk group stratification in the children's Oncology Group. *J Clin Oncol*. 2005;23:6459-6465.
4. Zaman S, Chobrutskiy BI, Blanck G. MAPT (Tau) expression is a biomarker for an increased rate of survival in pediatric neuroblastoma. *Cell Cycle*. 2018;17:2474-2483.
5. Zhou K, Li XL, Pan J, Xu JZ, Wang J. Analysis of the risk factor for the poor prognosis of localized neuroblastoma after the surgical. *Medicine*. 2018;97:e12718.
6. Beltran H. The N-myc oncogene: maximizing its targets, regulation, and therapeutic potential. *Mol Cancer Res*. 2014;12:815-822.
7. Kaur J, Debnath J. Autophagy at the crossroads of catabolism and anabolism. *Nat Rev Mol Cell Biol*. 2015;16:461-472.
8. Nassour J, Radford R, Correia A, et al. Autophagic cell death restricts chromosomal instability during replicative crisis. *Nature*. 2019;565:659-663.
9. White E. Deconvoluting the context-dependent role for autophagy in cancer. *Nat Rev Cancer*. 2012;12:401-410.
10. Belounis A, Nyalendo C, Le Gall R, et al. Autophagy is associated with chemoresistance in neuroblastoma. *BMC Cancer*. 2016;16:891.
11. Tanimoto T, Tazawa H, Ieda T, et al. Elimination of MYCN-amplified neuroblastoma cells by telomerase-targeted oncolytic virus via MYCN suppression. *Mol Ther Oncolytics*. 2020;18:14-23.
12. Dong Y, Gong W, Hua Z, et al. Combination of rapamycin and MK-2206 induced cell death via autophagy and necroptosis in MYCN-amplified neuroblastoma cell lines. *Front Pharmacol*. 2020;11:31.
13. Li Z, Yang C, Li X, et al. The dual role of BI 2536, a small-molecule inhibitor that targets PLK1, in induction of apoptosis and attenuation of autophagy in neuroblastoma cells. *J Cancer*. 2020;11:3274-3287.
14. Lin MC, Lee YW, Tseng YY, et al. Honokiol induces autophagic apoptosis in neuroblastoma cells through a p53-dependent pathway. *Am J Chin Med*. 2019;47:895-912.
15. Meng X, Li H, Fang E, Feng J, Zhao X. Comparison of stage 4 and stage 4s neuroblastoma identifies autophagy-related gene and LncRNA signatures associated with prognosis. *Front Oncol*. 2020;10:1411.
16. Yu G, Wang LG, Han Y, He QY. clusterProfiler: an R package for comparing biological themes among gene clusters. *OMICS*. 2012;16:284-287.
17. Wang X, Yao S, Xiao Z, et al. Development and validation of a survival model for lung adenocarcinoma based on autophagy-associated genes. *J Transl Med*. 2020;18:149.
18. Wolbers M, Koller MT, Witteman JC, Steyerberg EW. Prognostic models with competing risks: methods and application to coronary risk prediction. *Epidemiology*. 2009;20:555-561.
19. Alba AC, Agoritsas T, Walsh M, et al. Discrimination and calibration of clinical prediction models: users' guides to the medical literature. *JAMA*. 2017;318:1377-1384.
20. Huang M, Weiss WA. Neuroblastoma and MYCN. *Cold Spring Harb Perspect Med*. 2013;3:a014415-a014415.
21. Rusmini P, Cortese K, Crippa V, et al. Trehalose induces autophagy via lysosomal-mediated TFEB activation in models of motoneuron degeneration. *Autophagy*. 2019;15:631-651.
22. Vucicevic L, Misirkic M, Ciric D, et al. Transcriptional block of AMPK-induced autophagy promotes glutamate excitotoxicity in nutrient-deprived SH-SY5Y neuroblastoma cells. *Cell Mol Life Sci*. 2020;77:3383-3399.
23. Roberts SS, Mori M, Pattee P, et al. GABAergic system gene expression predicts clinical outcome in patients with neuroblastoma. *J Clin Oncol*. 2004;22:4127-4134.
24. Xiao W, Xiong Z, Yuan C, et al. Low neighbor of brca1 gene expression predicts poor clinical outcome and resistance of sunitinib in clear cell renal cell carcinoma. *Oncotarget*. 2017;8:94819-94833.
25. Marsh T, Kenific CM, Suresh D, et al. Autophagic degradation of NBR1 restricts metastatic outgrowth during mammary tumor progression. *Dev Cell*. 2020;52:591-604.e6.
26. Marsh T, Debnath J. Autophagy suppresses breast cancer metastasis by degrading NBR1. *Autophagy*. 2020;16:1164-1165.
27. Panigrahi DP, Praharaj PP, Bhol CS, et al. The emerging, multifaceted role of mitophagy in cancer and cancer therapeutics. *Semin Cancer Biol*. 2020;66:45-58.
28. Li C, Zhang Y, Cheng X, et al. PINK1 and PARK2 suppress pancreatic tumorigenesis through control of mitochondrial iron-mediated immunometabolism. *Dev Cell*. 2018;46:441-455.e8.
29. Yin K, Lee J, Liu Z, et al. Mitophagy protein PINK1 suppresses colon tumor growth by metabolic reprogramming via p53 activation and reducing acetyl-coa production. *Cell Death Differ*. 2021;28:2421-2435.
30. Simon AG, Tolkach Y, Esser LK, et al. Mitophagy-associated genes PINK1 and PARK2 are independent prognostic markers of survival in papillary renal cell carcinoma and associated with aggressive tumor behavior. *Sci Rep*. 2020;10:18857.
31. Lu X, Liu QX, Zhang J, et al. PINK1 overexpression promotes cell migration and proliferation via regulation of autophagy and predicts a poor prognosis in lung cancer cases. *Cancer Manag Res*. 2020;12:7703-7714.